Letter

Synthesis of Itaconic Acid Ester Analogs via Self-aldol Condensation of Ethyl Pyruvate Catalyzed by Hafnium BEA Zeolites

Yuran Wang, Jennifer D. Lewis, and Yuriy Roman-Leshkov

ACS Catal., **Just Accepted Manuscript** • DOI: 10.1021/acscatal.6b00561 • Publication Date (Web): 21 Mar 2016

Synthesis of Itaconic Acid Ester Analogs via Self-aldol Condensation of Ethyl Pyruvate Catalyzed by Hafnium BEA Zeolites

Yuran Wang, Jennifer D. Lewis and Yuriy Román-Leshkov*

Department of Chemical Engineering, Massachusetts Institute of Technology, Cambridge, MA 02139, US.

KEYWORDS: Itaconic acid ester, aldol condensation, pyruvate, hafnium beta, sodium exchange, open sites, Lewis acidic zeolites

ABSTRACT: Lewis acidic zeolites are used to synthesize unsaturated dicarboxylic acid esters via aldol condensation of keto esters. Hafnium-containing BEA (Hf-BEA) zeolites catalyze the condensation of ethyl pyruvate into diethyl 2-methyl-4-oxopent-2-enedioate and diethyl 2-methylene-4-oxopentanedioate (an itaconic acid ester analog) with a selectivity of ca. 80% at ca. 60% conversion in a packed-bed reactor. The catalyst is stable for 132 h on stream, reaching a turnover number of 5110 mol_{EP} mol_{Hf}^{-1}. Analysis of the dynamic behavior of Hf-BEA under flow conditions and studies with Na-exchanged zeolites suggest that Hf(IV) open sites possess dual functionality for Lewis and Brønsted acid catalysis.

Dicarboxylic acids (diacids) play a central role in the biobased chemicals portfolio, as evidenced by their prevalence in the top 12 chemicals from biomass identified by the U.S. Department of Energy.[1] Diacids are building blocks in condensation polymerization reactions,[2] and their ester forms (diesters) can serve as lubricants, plasticizers, and polymer intermediates.[3] In particular, the unsaturated diacid itaconic acid is a potential biodegradable substitute for high-volume petroleum-derived chemicals such as acrylic acid, maleic anhydride, or acetone cyanohydrin.[4] It can also be used in the production of superabsorbent polymers, synthetic latex, and laminating resins.[4] Although some diacids (e.g. succinic acid) are already produced industrially from biomass, most, including itaconic acid, suffer from prohibitively high production costs.[5-8] Current catalytic routes to synthesize diacids and diesters from biomass-derived molecules, such as Baeyer-Villiger oxidation,[9,10] C-C bond cleavage,[11] and noble metal catalyzed aerobic oxidation,[12,13] suffer from poor selectivity,[9,10] inefficient carbon utilization,[11] and/or catalyst deactivation.[12] Flanagan et al. reported a C-C coupling strategy to produce unsaturated dicarboxylic esters through the addition dimerization of crotonates;[14] however, the system depends on homogeneous catalysts.

An alternative route to generate diacids or diesters is via the C-C coupling of keto acids or esters (Scheme 1), which are common intermediates in a myriad of metabolic pathways and can be produced through biocatalysis on a large scale.[7,15-20] While this coupling strategy is promising, only a few homogeneous catalysts have been shown to activate the carbonyl group adjacent to the ester group.[21-23] However, these catalysts lactonize the aldol adducts instead of generating linear condensation products. Solid base catalysts typically used for aldol condensation are not ideal for the proposed system, as they easily deactivate in the presence of organic acids.[24-26]

In this work, we demonstrate a general strategy to synthesize unsaturated dicarboxylic acid esters via the C-C coupling of keto esters with Lewis acidic zeolites. We emphasize the synthesis of itaconic acid ester analogs from the condensation of ethyl pyruvate (EP, **1**) (Scheme 1) due to the low thermal stability of pyruvic acid.[27] Zeolites with BEA topology containing Lewis acidic framework heteroatoms, including Sn(IV), Hf(IV) and Zr(IV), can catalyze C-C coupling of biomass-derived oxygenates.[28-31] These materials promote aldol condensation via a soft enolization pathway reminiscent to that observed in type II aldolases.[24] Importantly, these zeolites feature remarkable tolerance to carboxylic acid groups[24] and water,[32,33] making them prime candidates for the biomass-based production of diacids and diesters.

Scheme 1. Self-aldol condensation of ethyl pyruvate catalyzed by Lewis acidic zeolites with products from side reactions listed

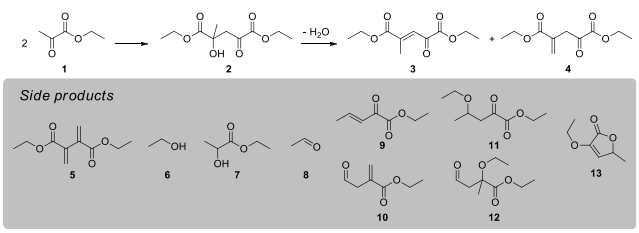

As depicted in Scheme 1, the self-aldol condensation of EP **1** followed by dehydration of the aldol addition product, diethyl 2-hydroxy-2-methyl-4-oxopentanedioate **2**, results in two diester isomers: diethyl 2-methyl-4-oxopent-2-enedioate **3** and diethyl 2-methylene-4-oxopentanedioate **4**. The latter is a functional analog of

itaconic acid ester. In addition to the main coupling reaction, several undesired side reactions are triggered by the presence of acid sites and water generated from the dehydration of aldol adducts. These side reactions (Scheme S1) include hydrolysis of EP to pyruvic acid and ethanol, Meerwein–Ponndorf–Verley (MPV) reduction of EP accompanied with Oppenauer oxidation of ethanol, and aldol reaction between EP and these side products. Toluene was used as the solvent to suppress side reactions that can occur between EP and alcohols (MPV) or water (hydrolysis).

Table 1. Self-aldol condensation of ethyl pyruvate catalyzed by Lewis acidic zeolites[a]

Entry	Catalyst	EP conversion (%)	Selectivity (%)[b] Diesters	Side products
1	Hf-BEA	80	68	15
2	Zr-BEA	81	64	11
3	Sn-BEA	19	67	6
4	Hf-BEA[c]	78	81	9

[a] Reaction conditions: 3 wt% EP in toluene, EP/metal = 195 (mol/mol), 120 °C, 1 h. [b] $Selectivity = \frac{\sum_i N_{C,i} n_i}{N_{C,EP}\left(n_{EP,o} - n_{EP}\right)} \times 100\%$, where $N_{C,i}$ is the number of carbon atoms in compound i, n_i is the number of moles of compound i in the reaction mixture, and $n_{EP,o}$ is the initial moles of EP added. Diesters: **3** - **5** in Scheme 1. Side products: **6** - **13** in Scheme 1; distribution for a typical reaction is shown in Figure S7. [c] Calcined in dry air at 550 °C for 5 h after four consecutive runs as shown in Figure S8.

The catalytic performance of Lewis acidic zeolites for the self-aldol condensation of EP is shown in Table 1. Hf-BEA and Zr-BEA generate the highest EP conversions (>80%) with comparable selectivities (>64%) to diester products (**3** - **5** in Scheme 1) after 1 h at 120 °C (entries 1 and 2). Sn-BEA shows a lower EP conversion of 19% under identical conditions (entry 3), consistent with previous studies on aldol reactions.[24] Only a ca. 1% conversion is observed from Si-BEA or metal oxides supported on Si-BEA, and a 17% conversion (with 12% selectivity) is obtained for Al-BEA (Table S1, entries 1-7). Collectively, these results indicate that the catalytic activity most likely originates from framework Lewis acidic heteroatoms. In contrast to previously reported homogeneous catalytic systems,[21-23] the lactonization of **2** is not observed with these Lewis acidic zeolites. Nonetheless, compound **13** is likely produced from the lactonization of a C7 molecule (reaction **f** in Scheme S1), indicating that although lactonization is feasible, the confining effects of the zeolite pores may limit this pathway for larger molecules.[34] Metal oxides with Brønsted basicity typically employed for aldol reactions, including MgO and hydrotalcite,[35] show EP conversions of less than 13% and selectivities of less than 18% (Table S1, entries 8-12). In these systems, pyruvic acid produced by the hydrolysis of EP is expected to deactivate the basic sites.[24]

Hf-BEA was investigated in further detail due to its superior diester selectivity (68%) at high conversion (80%). The recyclability of Hf-BEA was probed by washing with toluene and reusing the material for five consecutive batch reactions at 120 °C. After a gradual conversion decrease from 80% (run 1) to 60% (run 4), the catalyst shows no further conversion drop in run 5 (Figure S8). Remarkably, calcination of the catalyst under dry air after run 4 improves the diester selectivity from 68% to 81% in addition to recovering the initial activity (Table 1, entry 4). This unique behavior prompted us to further investigate the stability and regeneration of Hf-BEA for EP coupling under flow conditions.

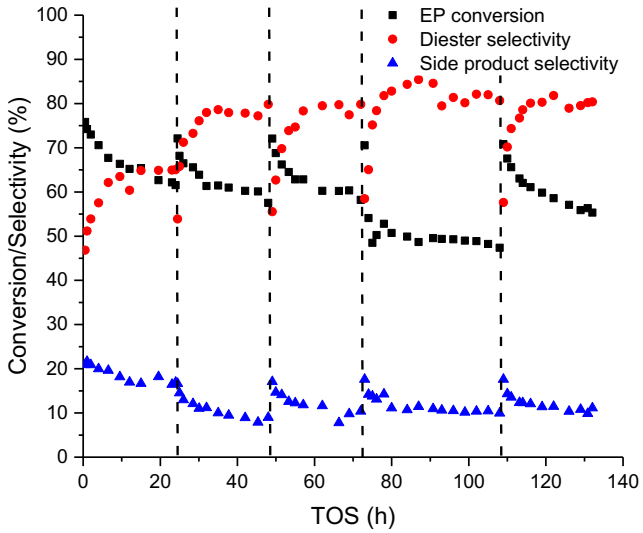

Figure 1. EP conversion and selectivity to diesters and side products as a function of time on stream (TOS) for the flow reaction with Hf-BEA. Reaction conditions: 120 °C, 12 bar, 320 mg Hf-BEA, 3 wt% EP in toluene, flow rate 0.20 mL min^{-1}, WHSV 32.2 h^{-1}. Dashed lines represent regeneration of Hf-BEA: flush with toluene at 120 °C, dry under N_2 at 150 °C, and calcine with dry air at 550 °C for 5 h. Diesters: **3** - **5** in Scheme 1. Side products: **6** - **13** in Scheme 1; distributions are shown in Figure S9.

Figure 1 shows EP conversion and selectivities to diesters and side products catalyzed by Hf-BEA as a function of time on steam (TOS) in a packed bed reactor (see Figure S10 for yields). Hf-BEA was calcined in situ under dry air at 550 °C for 5 h prior to feeding the reactants. The catalyst bed was regenerated by calcination under identical conditions over the course of the experiment; each cycle is indicated by the dashed lines in Figure 1. The reactor was operated at 120 °C with a weight hourly space velocity (WHSV) of 32.2 h^{-1}. Steady-state conversions of ca. 60%, selectivities towards diesters of ca. 80%, and a total turnover number of 5110 mol_{EP} mol_{Hf}^{-1} over 132 h on stream were observed. Elemental analysis of the spent catalyst showed no detectable change in Hf content (Table S3), and powder X-ray diffraction confirmed that the long-range crystallinity was preserved (Figure S13). N_2 adsorption data of the spent catalyst showed a slightly smaller micropore volume (0.17 cm^3 g^{-1}) than that of the pristine catalyst (0.19 cm^3 g^{-1}) (Table S3, Figure S16).

After each calcination, transient and steady-state regimes are clearly observed in the reactivity data (Figure 1

and Figure S10). During the transient periods, the EP conversion decreases by ca. 10% over 10 h TOS, while the diester selectivity increases by ca. 20% and the selectivity to side products decreases by ca. 5%. The decrease in EP conversion and the increase in diester selectivity appear to be correlated with a decrease in the rates of side reactions that are initiated by hydrolysis (Scheme S1), indicating the deactivation of active sites responsible for hydrolysis reactions. The steady-state period, which accounts for the remaining 14-26 h on stream, is characterized by less than 5% decrease in EP conversion and stable selectivity to diesters (Figure 1). Calcination of the catalyst bed results in a partial recovery of hydrolysis activity, demonstrating that deactivation of hydrolysis active sites is partially reversible. The regeneration by calcination coupled with the 5 wt% loss observed by thermogravimetric analysis of the catalyst recovered after 132 h TOS suggests that interaction of organic molecules with the sites contributes to the apparent decrease in hydrolysis rates.

The increased diester yield coupled with the concurrent decrease of hydrolysis activity in the transient regimes suggests that different moieties in the active site ensemble catalyze the aldol condensation and hydrolysis reactions. Control batch reactions with Si-BEA (Table S1, entries 4-5) showed no activity, thus pointing to the involvement of Hf in generating these sites. In addition to Lewis acidity, spectroscopic evidence[36] and computational studies[37-39] suggest the presence of weak Brønsted acidity associated with the silanol moiety of monohydrolyzed framework heteroatom sites (i.e. open sites) in Lewis acidic zeolites. Thus, these weak Brønsted acid sites are likely responsible for hydrolysis, and selective deactivation of the acidic proton due to alkoxide formation could explain the transient deactivation of hydrolysis. Indeed, similar deactivation behavior has been observed in the flow studies of Lewis acidic zeolites.[40,41] Lewis et al. showed through Sn- or Hf-BEA catalyzed tandem reactions between 5-(hydroxymethyl)furfural and alcohols that Lewis acid-catalyzed transfer hydrogenation activity remained unchanged, while Brønsted acid-catalyzed etherification activity decreased over time and could be partially recovered by calcination.[40] Importantly, $^{13}C\{^1H\}$ CP MAS NMR of the spent catalyst showed alkoxide species formation on silanol groups in the zeolite.[40]

An important feature demonstrated in the flow data is the increase in selectivity toward diesters after the first regeneration by calcination (Figure 1, after 24 h TOS) that is consistent with the increase in selectivity observed after calcination in the batch studies. Specifically, the steady-state diester selectivity increases from 65% to 79% (yield: 42% to 48%), and the steady-state selectivity to side products decreases from 17% to 10% (yield: 11% to 5%). However, no further improvement in diester selectivity is observed after successive calcinations. This irreversible shift in selectivity after the first regeneration is indicative of permanent changes to the catalyst active sites that contribute to the decrease in hydrolysis activity, the increase in aldol condensation activity, or a combination of both.

The dynamic behavior exhibited by Hf-BEA in flow is consistent with prior studies of Lewis acidic zeolites that suggest amorphization and site restructuring are responsible for changes in activity and selectivity after extended TOS.[30,40,41] Specifically, for aqueous dihydroxyacetone isomerization, Lari et al. observed an 18% loss in crystallinity for Sn-BEA and a 16% decrease in tetrahedral coordination for Sn-MFI after 24 h TOS.[41] Lewis et al. demonstrated with ^{119}Sn MAS and $^{119}Sn\{^1H\}$ CP/MAS NMR that open and distorted framework Sn sites were generated in ^{119}Sn-BEA during the transfer hydrogenation and etherification of 5-(hydroxymethyl)furfural with ethanol, while only closed sites were observed in the pristine catalyst.[40] Studies by Boronat et al. and Bermejo-Deval et al. also suggest that the distribution of open and closed sites in Sn-BEA changes with post-synthesis treatment, e.g. calcination or exposure to reaction conditions.[42,43]

The molecular connectivity of active sites, i.e. open versus closed, has been suggested to affect catalytic activity and selectivity due to differences in Lewis acidity, flexibility, and functionality of the neighboring silanol group.[42-46] Bermejo-Deval et al. demonstrated with Na-treated Sn-BEA that the cations likely exchange onto silanol groups proximal to Sn(IV) open sites.[45] The presence of Na^+ alters the glucose isomerization reaction pathway from a fructose-producing 1,2-hydride shift to a mannose-producing 1,2-carbon shift, and the effect can be reversed by washing with a H_2SO_4 solution to remove the Na^+ cations.[45] Computational studies indicate that the change in product distribution is a consequence of the electrostatic stabilization of the carbon shift relative to hydride shift caused by the presence of Na^+ ions at the open Sn center.[47] To probe the nature of the active sites in Hf-BEA, we conducted a preliminary study with Na-exchanged Hf-BEA. Specifically, two Na-exchanged Hf-BEA catalysts were prepared using methods adapted from the work of Bermejo-Deval et al. (see Section S1).[45] These samples were denominated as Hf-BEA-Na-1 and Hf-BEA-Na-2, with Na/Hf molar ratios of 0.69 and 0.02, respectively (Table 2). Batch reactions catalyzed by Hf-BEA-Na-1 resulted in 15% EP conversion and ca. 34% selectivity to diesters (Table 2 and S2, entry 2). This significant reduction in activity and selectivity is unlikely a result of pore blockage (Section S2). Despite its low Na content, Hf-BEA-Na-2 resulted in a diminished EP conversion of 59% when compared to the 77% conversion generated by pristine Hf-BEA (Tables 2 and S2, entry 3). The catalyst performance and pore volume of both Na-exchanged zeolites were recovered by washing with H_2SO_4 (Tables 2 and S2, entries 4-5). This reversible activity drop is likely caused by a strong interaction between Na^+ and the active sites, which we investigate further using Fourier transform infrared (FTIR) spectroscopy with deuterated acetonitrile (CD_3CN) adsorption.

FTIR spectra of CD_3CN adsorbed on pristine Hf-BEA show the characteristic bands seen with M-BEA zeolites (Figure 2a).[42,45,48] The C≡N stretching vibrations of CD_3CN at 2310 cm^{-1}, 2275 cm^{-1}, and 2268 cm^{-1} are representative of CD_3CN that is strongly bound to Lewis acid sites (i.e. tetrahedral Hf(IV) centers), coordinated to silanol groups,

Table 2. Aldol condensation of ethyl pyruvate catalyzed by Na-exchanged and acid-washed Hf-BEA[a]

Entry	Cat.	Treatment	Si/Hf ratio[c]	Na/Hf molar ratio[d]	Micropore volume ($cm^3\ g^{-1}$)	EP conv. (%)	Selectivity (%)[b] Diesters	Side products
1	Hf-BEA	None	115	n/a	0.20	77	69	7
2	Hf-BEA-Na-1[e]	$NaNO_3$ (1 M)	116	0.69	0.17	15	34	10
3	Hf-BEA-Na-2[f]	NaOH (pH = 10)	113	0.02	0.20	59	70	7
4	Hf-BEA-AW-1[g]	H_2SO_4 (1 M)	115	n.d.	0.20	74	69	12
5	Hf-BEA-AW-2[g]	H_2SO_4 (1 M)	119	n.d.	0.19	77	79	7

[a] Reaction conditions same as in Table 1, but with a different batch of Hf-BEA zeolite. [b] Selectivity same as defined in Table 1. [c] No significant changes in Si/Hf ratios after different treatments, indicating the treatments do not cause Hf leaching. [d] n/a, not applicable. n.d., not detected. [e] Hf-BEA after Na exchange treatment 1 with $NaNO_3$ (1 M). [f] Hf-BEA after Na exchange treatment 2 with NaOH (pH =10). [g] Hf-BEA-Na-1 or Hf-BEA-Na-2 washed with H_2SO_4 (1 M) at room temperature for 1 h, recovered and then calcined at 550 °C. Full details on material synthesis available in Section S1.

and physisorbed, respectively.[42,45] The band at 2310 cm^{-1} appears to be a single peak, which differs from previous reports of two bands corresponding to open and closed sites for Sn-BEA.[42,45] However, these data are consistent with studies of Zr-BEA that show only one band in this region.[36] Na exchange results in a decrease in the band at 2310 cm^{-1} and the appearance of a new band at 2284 cm^{-1}, which has previously been assigned as CD_3CN adsorbed on Na-exchanged open sites for Sn-BEA.[45] This change is more prominent for the material with a higher degree of Na exchange (Hf-BEA-Na-1, Figure 2b) than for the material with low Na loading (Hf-BEA-Na-2, Figure S18a). Controls with Na-exchanged Si-BEA (Si-BEA-Na) confirm that framework Hf(IV) is required to observe this feature (Figure S18b).[49] After acid wash, the FTIR spectra resemble again those of the pristine material, demonstrating the reversibility of the Na exchange (Figure 2c).

Assuming that Na^+ interacts with the open framework Hf(IV) site in a similar manner to that proposed by Bermejo-Deval et al. for Sn-BEA,[45] we hypothesize that the open sites are the main active sites for aldol condensation. Thus, open site ensembles likely have twofold functionality: the Lewis acidic character of the heteroatom catalyzes aldol reaction, while the Brønsted acidic silanol group catalyzes hydrolysis. The change in the chemical environment of the open site upon Na exchange—evidenced by the change in the FTIR band corresponding to CD_3CN adsorbed on Hf sites from 2310 to 2284 cm^{-1}—may explain the lower reactivity of Na-exchanged Hf-BEA for aldol condensation. However, the presence and catalytic contribution of Hf(IV) closed sites cannot be excluded. Detailed characterization and kinetics studies are currently underway to confirm these hypotheses.

In summary, we have developed a new approach to synthesize unsaturated dicarboxylic acid esters from keto esters via aldol condensation catalyzed by Lewis acidic zeolites. In particular, we demonstrate that Hf-BEA can catalyze the self-aldol condensation of EP in toluene to produce itaconic acid ester analogs. The catalyst is stable for 132 h TOS in a packed-bed reactor with a diester selectivity of ca. 80% at 120 °C. Na exchange substantially decreases Hf-BEA activity and significantly alters the FTIR band for $CDCN_3$ adsorbed on the framework Hf(IV) sites, indicating a strong interaction between Na^+ and the active sites. The open framework Hf(IV) site is hypothesized to possess strong Lewis acidity and weak Brønsted acidity that are responsible for the dual functionality of the catalyst. However, further investigation is needed to fully elucidate the nature of the active site and guide catalyst and reaction optimization.

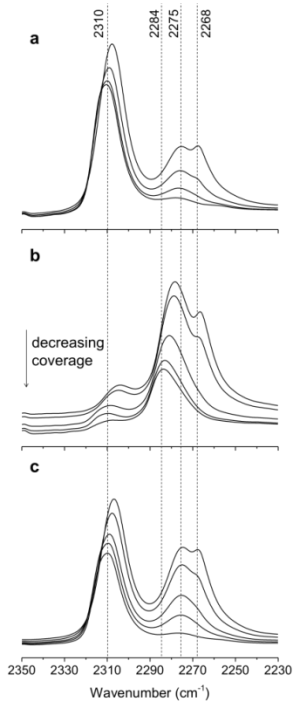

Figure 2. FTIR spectra with decreasing CD_3CN coverage on a) Hf-BEA, b) Hf-BEA-Na-1, and c) Hf-BEA-AW-1. Signals are referenced to the bare material and normalized by the combination and overtone modes of zeolite Si-O-Si stretches (1750–2100 cm^{-1}). Reference lines are for physisorbed CD_3CN (2268 cm^{-1}) and CD_3CN adsorbed on silanols (2275 cm^{-1}), Na-exchanged open Hf(IV) sites (tentative, 2284 cm^{-1}), and Lewis acidic Hf sites (2310 cm^{-1}).

ASSOCIATED CONTENT

Supporting Information

The supporting information includes experimental procedures for catalyst synthesis, characterization, and test reactions, side reaction scheme, a typical GC chromatogram for reaction mixtures, MS data for reaction products, additional reaction data for batch studies, flow studies and Na exchange studies, and catalyst characterization data (ICP-MS, PXRD, N_2 adsorption-desorption and FTIR). This material is available free of charge via the Internet at http://pubs.acs.org.

AUTHOR INFORMATION

Corresponding Author

*Email: yroman@mit.edu.

Notes

The authors declare no competing financial interest.

ACKNOWLEDGMENT

This work was sponsored by the Chemical Sciences, Geosciences and Biosciences Division, Office of Basic Energy Sciences, Office of Science, U.S. Department of Energy, under Award No. DE-FG0212ER16352. J.D.L. was partially supported by the National Science Foundation Graduate Research Fellowship under Grant No. 122374. Any opinion, findings, and conclusions or recommendations expressed in this material are those of the authors and do not necessarily reflect the views of the National Science Foundation.

ABBREVIATIONS

Diacids, dicarboxylic acids; diesters, dicarboxylic acid esters; C-C, carbon-carbon; EP, ethyl pyruvate; MPV reduction, Meerwein–Ponndorf–Verley reduction; TOS, time on stream; WHSV, weight hourly space velocity; FTIR, Fourier transform infrared spectroscopy; CP, cross polarization; MAS, magic-angle spinning; NMR, nuclear magnetic resonance.

REFERENCES

(1) Werpy, T.; Petersen, G.; Aden, A.; Bozell, J.; Holladay, J.; White, J.; Manheim, A.; Eliot, D.; Lasure, L.; Jones, S. "Top value added chemicals from biomass. Volume 1-Results of screening for potential candidates from sugars and synthesis gas," Department of Energy Washington DC, 2004.

(2) Dicarboxylic Acids, Aliphatic. Ullmann's Encyclopedia of Industrial Chemistry [Online]; Wiley-VCH Verlag GmbH & Co. KGaA, Posted NOV 19, 2014. http://onlinelibrary.wiley.com/doi/10.1002/14356007.a08_523.pub3/pdf.

(3) Dicarboxylic Acids. Kirk-Othmer Encyclopedia of Chemical Technology [Online]; John Wiley & Sons, Inc., Posted Sep 17, 2010. http://onlinelibrary.wiley.com/doi/10.1002/0471238961.0409030110150814.a01.pub2/pdf.

(4) "Towards a sustainable bio-industry -- Biotechnology for renewable chemicals and innovative downstream processes," WEASTRA s.r.o., 2012.

(5) Okabe, M.; Lies, D.; Kanamasa, S.; Park, E. Y. *Appl. Microbiol. Biotechnol.* **2009,** *84*, 597-606.

(6) Steiger, M. G.; Blumhoff, M. L.; Mattanovich, D.; Sauer, M. *Front. Microbiol.* **2013,** *4*, 23.

(7) Straathof, A. J. *Chem. Rev.* **2014,** *114*, 1871-1908.

(8) Mondala, A. H. *J. Ind. Microbiol. Biotechnol.* **2015,** *42*, 487-506.

(9) Wang, Y. R.; Vogelgsang, F.; Roman-Leshkov, Y. *ChemCatChem* **2015,** *7*, 916-920.

(10) Dutta, S.; Wu, L. L.; Mascal, M. *Green Chem.* **2015,** *17*, 2335-2338.

(11) Liu, J.; Du, Z.; Lu, T.; Xu, J. *ChemSusChem* **2013,** *6*, 2255-2258.

(12) Wang, Y. R.; Van de Vyver, S.; Sharma, K. K.; Roman-Leshkov, Y. *Green Chem.* **2014,** *16*, 719-726.

(13) Casanova, O.; Iborra, S.; Corma, A. *ChemSusChem* **2009,** *2*, 1138-1144.

(14) Flanagan, J. C. A.; Kang, E. J.; Strong, N. I.; Waymouth, R. M. *ACS Catal.* **2015,** *5*, 5328-5332.

(15) Wieschalka, S.; Blombach, B.; Bott, M.; Eikmanns, B. J. *Microb. Biotechnol.* **2013,** *6*, 87-102.

(16) Li, Y.; Chen, J.; Lun, S. Y. *Appl. Microbiol. Biotechnol.* **2001,** *57*, 451-459.

(17) Schwartz, T. J.; Shanks, B. H.; Dumesic, J. A. *Curr. Opin. Biotechnol.* **2016,** *38*, 54-62.

(18) Dusselier, M.; Van Wouwe, P.; Dewaele, A.; Makshina, E.; Sels, B. F. *Energ. Environ. Sci* **2013,** *6*, 1415-1442.

(19) Il'Chenko, A.; Shcherbakova, V. *Microbiology* **2008,** *77*, 430-435.

(20) Johnson, C. W.; Beckham, G. T. *Metab. Eng.* **2015,** *28*, 240-247.

(21) Gathergood, N.; Juhl, K.; Poulsen, T. B.; Thordrup, K.; Jorgensen, K. A. *Org. Biomol. Chem.* **2004,** *2*, 1077-1085.

(22) Dambruoso, P.; Massi, A.; Dondoni, A. *Org. Lett.* **2005,** *7*, 4657-4660.

(23) Wang, Q.; Sun, Y.; Chen, H.; Li, Z.; Tao, F. *Synthesis* **2008,** *2008*, 589-593.

(24) Lewis, J. D.; Van de Vyver, S.; Roman-Leshkov, Y. *Angew. Chem. Int. Ed. Engl.* **2015,** *54*, 9835-9838.

(25) Podrebarac, G. G.; Ng, F. T. T.; Rempel, G. L. *Chem. Eng. Sci.* **1997,** *52*, 2991-3002.

(26) *New Solid Acids and Bases: Their Catalytic Properties*; Tanabe, K.; Misono, M.; Ono, Y.; Hattori, H., Eds.; Elsevier Science Publishing Company, Inc.: New York, NY, 1989, p 339.

(27) Frey, H. "Thermal decomposition of pyruvic acid and its esters leading to CO_2," California. Univ., Berkeley. Radiation Lab', 1956.

(28) Mahmoud, E.; Yu, J. Y.; Gorte, R. J.; Lobo, R. F. *ACS Catal.* **2015,** *5*, 6946-6955.

(29) Van de Vyver, S.; Román-Leshkov, Y. *Angew. Chem. Int. Ed.* **2015,** *54*, 12554-12561.

(30) Van de Vyver, S.; Odermatt, C.; Romero, K.; Prasomsri, T.; Román-Leshkov, Y. *ACS Catal.* **2015,** *5*, 972-977.

(31) Holm, M. S.; Pagan-Torres, Y. J.; Saravanamurugan, S.; Riisager, A.; Dumesic, J. A.; Taarning, E. *Green Chem.* **2012,** *14*, 702-706.

(32) Moliner, M.; Roman-Leshkov, Y.; Davis, M. E. *Proc. Natl. Acad. Sci. U S A* **2010,** *107*, 6164-6168.

(33) Roman-Leshkov, Y.; Moliner, M.; Labinger, J. A.; Davis, M. E. *Angew. Chem. Int. Ed. Engl.* **2010,** *49*, 8954-8957.

(34) De Clercq, R.; Dusselier, M.; Christiaens, C.; Dijkmans, J.; Iacobescu, R. I.; Pontikes, Y.; Sels, B. F. *ACS Catal.* **2015,** *5*, 5803-5811.

(35) Sacia, E. R.; Balakrishnan, M.; Deaner, M. H.; Goulas, K. A.; Toste, F. D.; Bell, A. T. *ChemSusChem* **2015,** *8*, 1726-1736.

(36) Sushkevich, V. L.; Vimont, A.; Travert, A.; Ivanova, I. I. *J. Phys. Chem. C* **2015,** *119*, 17633-17639.

(37) Montejo-Valencia, B. D.; Salcedo-Pérez, J.; Curet-Arana, M. C. *J. Phys. Chem. C* **2016,** *120*, 2176-2186.

(38) Yang, G.; Zhou, L.; Han, X. *J. Mol. Catal. A: Chem.* **2012,** *363*, 371-379.

(39) Yang, G.; Lan, X. J.; Zhuang, J. Q.; Ma, D.; Zhou, L. J.; Liu, X. C.; Han, X. W.; Bao, X. H. *Appl. Catal., A* **2008,** *337*, 58-65.

(40) Lewis, J. D.; Van de Vyver, S.; Crisci, A. J.; Gunther, W. R.; Michaelis, V. K.; Griffin, R. G.; Roman-Leshkov, Y. *ChemSusChem* **2014,** *7*, 2255-2265.

(41) Lari, G.; Dapsens, P.; Scholz, D.; Mitchell, S.; Mondelli, C.; Pérez-Ramírez, J. *Green Chem.* **2016,** *18*, 1249-1260.

(42) Boronat, M.; Concepcion, P.; Corma, A.; Renz, M.; Valencia, S. *J. Catal.* **2005,** *234*, 111-118.
(43) Bermejo-Deval, R.; Assary, R. S.; Nikolla, E.; Moliner, M.; Roman-Leshkov, Y.; Hwang, S. J.; Palsdottir, A.; Silverman, D.; Lobo, R. F.; Curtiss, L. A.; Davis, M. E. *Proc. Natl. Acad. Sci. U S A* **2012,** *109*, 9727-9732.
(44) Sushkevich, V. L.; Palagin, D.; Ivanova, I. I. *ACS Catal.* **2015,** *5*, 4833-4836.
(45) Bermejo-Deval, R.; Orazov, M.; Gounder, R.; Hwang, S. J.; Davis, M. E. *ACS Catal.* **2014,** *4*, 2288-2297.
(46) Harris, J. W.; Cordon, M. J.; Di Iorio, J. R.; Vega-Vila, J. C.; Ribeiro, F. H.; Gounder, R. *J. Catal.* **2016,** *335*, 141-154.
(47) Christianson, J. R.; Caratzoulas, S.; Vlachos, D. G. *ACS Catal.* **2015,** *5*, 5256-5263.
(48) Roy, S.; Bakhmutsky, K.; Mahmoud, E.; Lobo, R. F.; Gorte, R. J. *ACS Catal.* **2013,** *3*, 573-580.
(49) Yu, J.; Luo, J.; Zhang, Y.; Cao, J.; Chang, C.-C.; Gorte, R.; Fan, W. *Microporous Mesoporous Mater.* **2016,** *225*, 472-481.

SYNOPSIS TOC

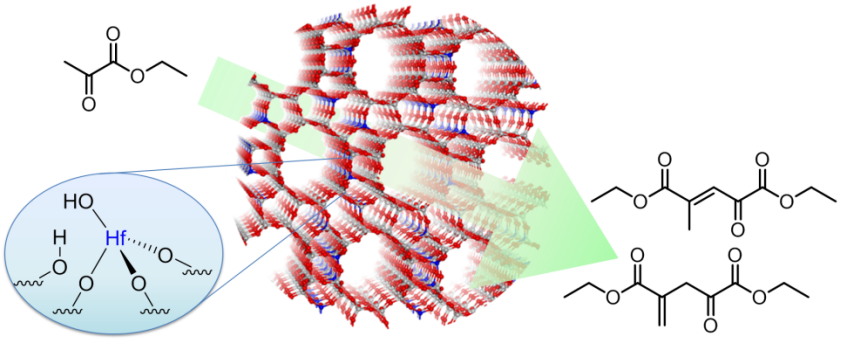

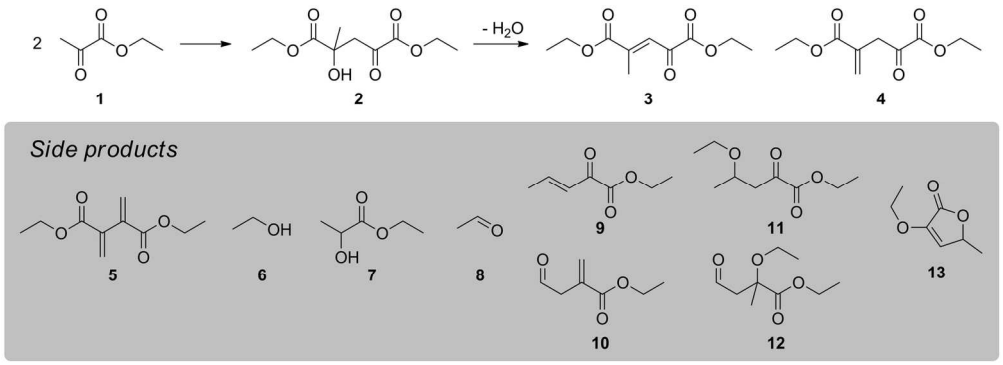

Scheme 1. Self-aldol condensation of ethyl pyruvate catalyzed by Lewis acidic zeolites with products from side reactions listed
77x27mm (600 x 600 DPI)

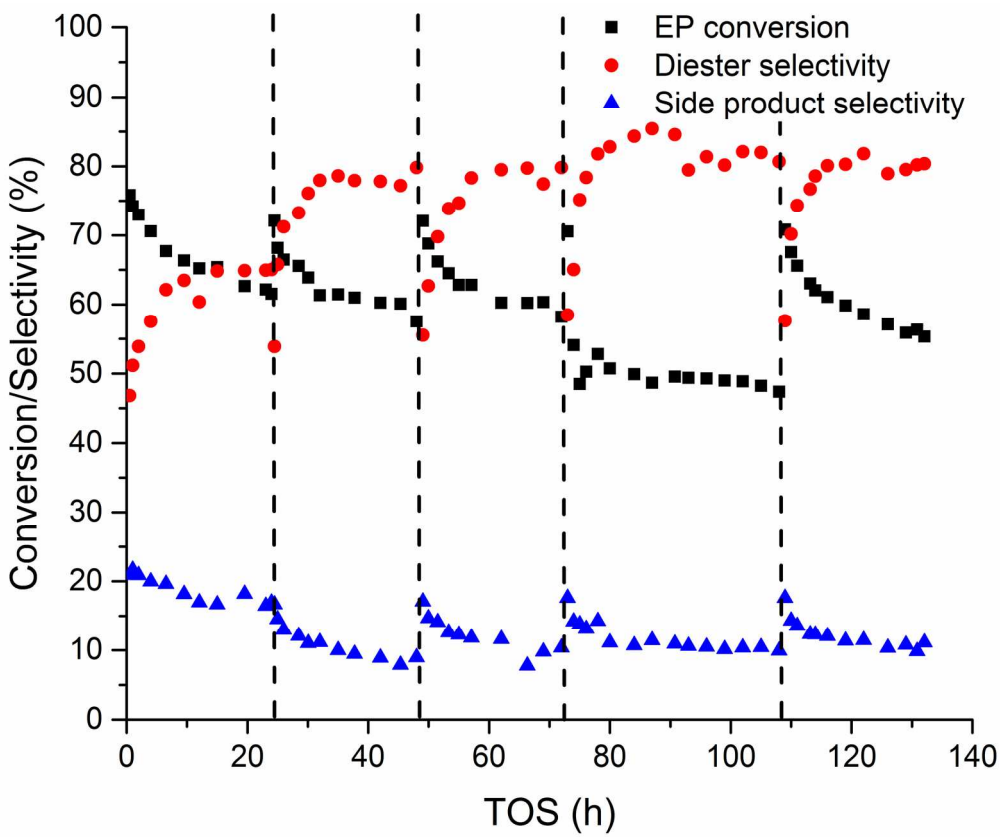

Figure 1. EP conversion and selectivity to diesters and side products as a function of time on stream (TOS) for the flow reaction with Hf-BEA. Reaction conditions: 3 wt% EP in toluene, 120 °C, 12 bar. Flow reactor operating conditions: 320 mg Hf-BEA, flow rate 0.20 mL min^{-1}, WHSV 32.2 h^{-1}. Dashed lines represent regeneration of Hf-BEA: flush with toluene at 120 °C, dry under N_2 at 150 °C and calcine with dry air at 550 °C for 5 h. Diesters: 3 - 5 in Scheme 1. Side products: 6 - 13 in Scheme 1; distributions are shown in Figure S9.
173x144mm (300 x 300 DPI)

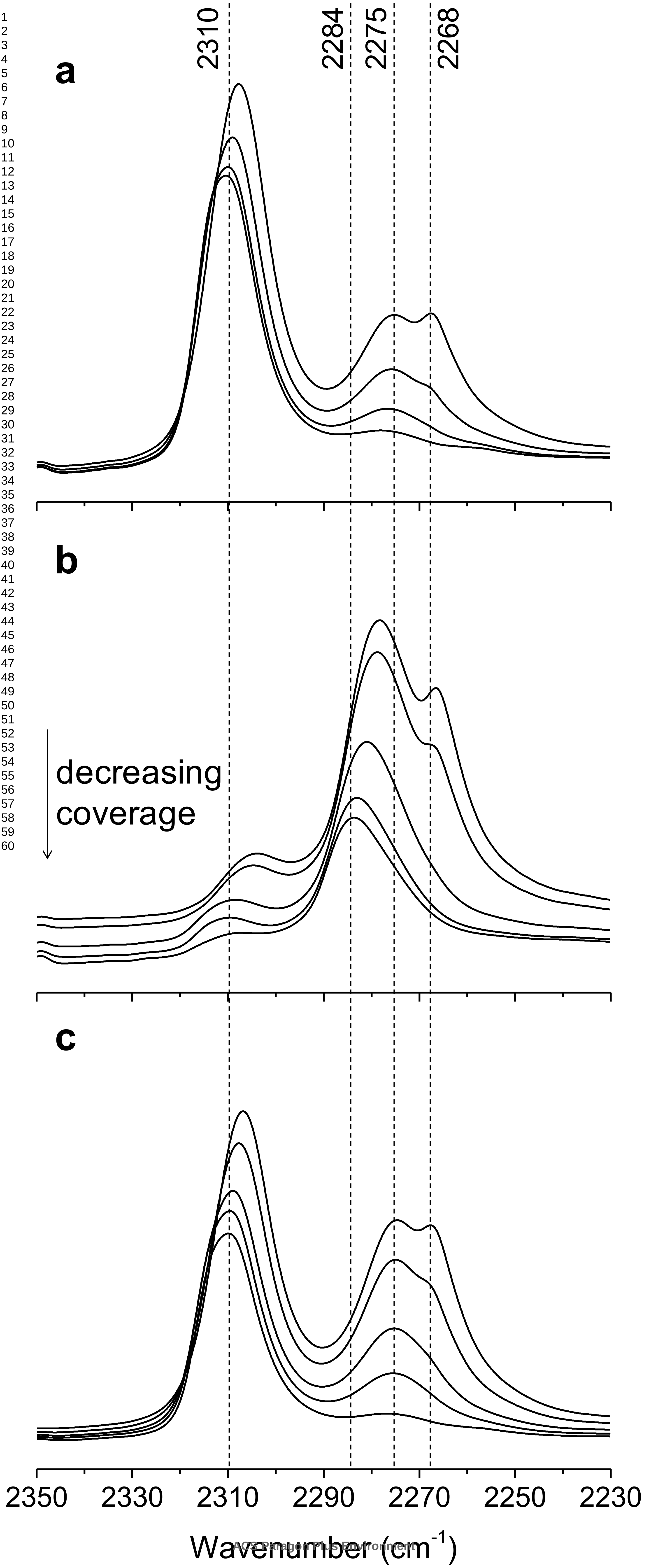
2310
2284
2275
2268
a
b
decreasing coverage
c
2350
2330
2310
2290
2270
2250
2230
Wavenumber (cm-1)

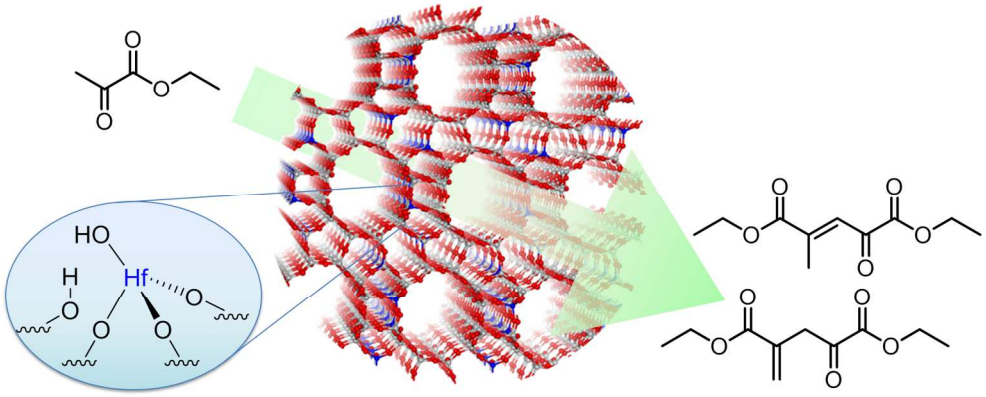

307x126mm (150 x 150 DPI)